Assessing future climate change in the Iberian Upwelling System

Ana Cordeiro Pires†, Rita Nolasco†, Alfredo Rocha† and Jesus Dubert†

†CESAM – Centre for Environmental and Marine Studies, University of Aveiro
Campus de Santiago, Departamento de Fisica, 3810-193 Aveiro, Portugal
anacpires@ua.pt
rita.nolasco@ua.pt
jdubert@ua.pt
alfredo.rocha@ua.pt

www.cerf-jcr.org

www.JCRonline.org

ABSTRACT

Cordeiro Pires, A., Nolasco, R., Rocha, A. and Dubert, J., 2013. Assessing future climate change in the Iberian Upwelling System, *Proceedings 12th International Coastal Symposium* (Plymouth, England), *Journal of Coastal Research*, Special Issue No. 65, pp. 1909-1914, ISSN 0749-0208.

The Western Iberian Margin is the northern limit of the Canary Upwelling System, a region of strong mesoscale activity, seasonal variability and thus very likely to be sensitive to climate change. Using a regional ocean model and data from several coupled global climate models (CGCM), climatological simulations were set up for present and for a future scenario. Forcing is obtained from averaging the outputs of an ensemble of CGCM provided by the Intergovernmental Panel for Climate Change (IPCC) A2 emission scenario. Results are focused on the continental shelf (~200 m). In general, the sea surface temperature (SST) seasonal evolution shows, for the future, an increase of about 1ºC during the upwelling season (April to September) and 2ºC in the rest of the year, while sea surface salinity (SSS) shows a freshening of about -0.2. These results agree with a general increase in air temperature and in fresh water input resulting from ice melting in the North Pole, which characterize this future scenario. However, differences depend on latitude and distance from the coast (higher differences to the south and more offshore, respectively). Also, SSS undergoes a shift of its minimum from July to May or September. Cross-shore sections show that SST and SSS differences are mainly observed in the upper 200 m. In winter, the typical upper slope poleward flow undergoes a slight weakening and shallowing. In summer, while the upwelling jet intensifies at the surface, it is also more restricted in both width and depth.

ADDITIONAL INDEX WORDS: *Regional ocean modeling, IPCC, dynamics, hydrography, seasonality.*

INTRODUCTION

The western coast of the Iberian Peninsula is the northernmost limit of the Eastern North Atlantic Upwelling System, also known as the Canary Upwelling System (Barton *et al*., 1998). In late spring and summer, due to the presence of the Azores high-pressure system, there are northerly winds along the coast of Western Iberian Margin (WIM). Northerly wind stress over the coastal ocean surface results in an offshore displacement of water through the Coriolis effect, which in turn forces deeper waters to upwell (Wooster et al., 1976). These colder waters are nutrient-rich and give rise to phytoplankton blooms, the reason why upwelling systems are the most productive regions of the world ocean (Pauly and Christensen, 1995). Upwelling also originates an associated equatorward jet (Peliz *et al*., 2002).

During winter, the surface and subsurface circulation off WIM is predominantly northwards because there is a general reversal of the wind regime. This poleward circulation, known as the Iberian Poleward Current (IPC), is typical of mid-latitude western coasts and consists of an upper slope/shelf break poleward flow driven by meridional alongshore density gradients that transports saltier and warmer (subtropical) waters (Peliz *et al*., 2005).

Due to the nature of these areas, upwelling systems are very important fisheries. Since these regions are already subject to intense seasonal and interannual variability, they are also potentially more sensitive to climate change (Holt *et al*., 2010). Early studies by Bakun (1990) postulated that a global increase in surface air temperature over land would intensify the land-sea pressure gradient at coastal regions, which in turn would cause an intensification of alongshore winds and subsequently upwelling. Upwelling intensification means cooling of the sea surface temperature (SST), which results in a positive feedback in the land-sea pressure gradient. Several works based on observations of SST time series for the last decades confirm this tendency for WIM (Santos *et al*., 2005; Relvas *et al*., 2009), while others postulate a weakening of the upwelling signal due to the general warming of SST (Lemos and Pires, 2004; Perez *et al*., 2010, both based on wind stress time series). As far as modeling studies are concerned, the Intergovernmental Panel for Climate Change (IPCC) future scenarios have been applied to the ocean in the past few years, but results vary widely. For instances, Mote and Mantua (2002) found no significant change in future years for any of the world upwelling systems, whereas Snyder *et al*. (2003) and Miranda *et al*. (2012) obtained results in agreement with Bakun (1990) for the California Current System and the Iberian Upwelling System, respectively.

This work consists in a case study of the impacts of a global climate change scenario on the hydrography and dynamics of the Iberian Upwelling System through numerical modeling, focusing on the continental shelf and upper slope of the western coast of the Iberian Peninsula. Using a nested regional configuration and a downscaling methodology, we compare the mean circulation features of the upper levels along WIM with the dynamics imposed by a set of atmospheric conditions dictated by a future

DOI: 10.2112/SI65-323.1 received Day Month 2012; accepted Day Month 2013.

atmospheric circulation regime. This data is obtained from the IPCC emission scenario A2 (Nakicenovic and Swart, 2000).

METHODS

Ocean Model

For the numerical simulations, we use the Regional Ocean Modeling System (ROMS) (Shchepetkin and McWilliams, 2005). ROMS is a split-explicit, free-surface, topography following coordinate model, designed to resolve regional problems. ROMS solves the primitive equations based on the Boussinesq and hydrostatic approximations. The numerical configuration is the same as the one used by Nolasco *et al*. (in review). It consists of an offline nesting configuration, where a medium-resolution mother domain, with climatological values on its boundaries, provides boundary and initial conditions to a high-resolution domain of the WIM (Figure 1). The First Domain (FD) has a horizontal resolution of 1/10º (~9 km) and 30 vertical levels, comprising the Azores Islands to the west, the Madeira Islands to the south and the Gulf of Biscay to the north. The target domain (Second Domain – SD), which has a resolution of 1/27º (~3 km), extends from the Gulf of Cadiz to the south, about 270 km off westwards and the Galician northern coast, and has 60 vertical levels. In allowing the running of two domains, we aim at more realistic conditions at play at the boundaries of the target domain and as little interference as possible of the boundaries of the first domain.

The climatologies used at the boundaries of FD are from the World Ocean Atlas 2009 (Locarnini *et al*., 2010; Antonov *et al*., 2010). These climatologies are used as the initial conditions for the temperature and salinity fields, and also to recycle these fields along the nudging bands, providing open boundary conditions. Since there are no projections for the future hydrography with the exception of the ocean surface, these climatologies are used in both the present and the future FD simulations. We consider this to be a valid approach because, from a climatological point of view, the deeper levels are less subject to atmospheric forcing than the first 200 m, which are the scope of this work. Furthermore, the effects of rising temperatures in the ocean at the depths of the intermediate and deep waters must have a much slower response than at the upper levels, such as this study means to illustrate.

In FD, the Mediterranean undercurrent is introduced as a nudging zone in the interior of the Gulf of Cadiz, as described by Peliz *et al*. (2007), in order to restore the hydrological properties at the Mediterranean levels. In SD, the water exchange with the Mediterranean basin is explicitly represented, consisting in the imposition of vertical profiles of temperature, salinity and zonal velocity at the Strait (Peliz *et al*., 2007).

The ROMS simulations are setup as such: each domain is run for ten years in order to check for stability in the kinetic energy of the system. The first five years of simulation of SD correspond to a period of spin-up, at which the Mediterranean Water is allowed to fully spread throughout the domain. The SD boundaries are forced with year five of the output of FD (other years were used as forcing and showed similar results). Surface forcing is described in the following sub-section.

Forcing Data

This study comprises the analysis of two ROMS climatological simulations, one for the present and one for the future. As surface forcing, ROMS requires heat fluxes (short-wave, long-wave and latent), water fluxes (evaporation minus precipitation), surface air temperature, humidity are obtained from the IPCC A2 emission

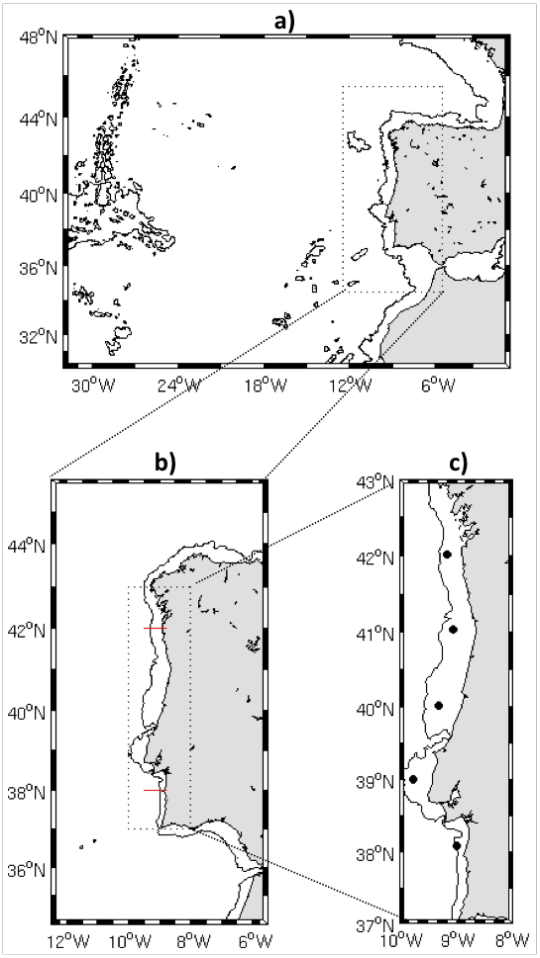

Figure 1. Area of study. (a) First Domain (FD) (2000-m isobath shown); (b) Second Domain (SD) with the sections of Figures 4 and 5 (200-m isobath shown); (c) points at which temperature and salinity are shown in Figure 2 (200-m isobath shown).

scenario (Nakicenovic and Swart, 2000). IPCC comprehends a large number of coupled global climate models (CGCM). The database can be found at the World Climate Research Programme (WCRP – http://www.wcrp-climate.org/) through the Coupled Model Intercomparison Project phase 3 (CMIP3) archived at the Program for Climate Model Diagnosis and Intercomparison (PCMDI) (http://www-pcmdi.llnl.gov/ipcc/about_ipcc.php). Nine CGCM had the variables needed and each variable was monthly averaged. These mean fields were then averaged to create an ensemble mean with which to force ROMS, for the present time and for the future. This method has been demonstrated as a good approach, since it minimizes the individual uncertainties of each model (Annan and Hargreaves, 2010). These nine models are listed in Table 1. Cordeiro Pires *et al*. (in prep) carried out a sensitivity study and showed that the ensemble mean is the most suitable forcing when comparing to climatological fields.

Present ensemble consists in monthly means of years 1945-1989 and future ensemble in monthly means of years 2071-2100. Period 1945-1989 was chosen in agreement with the climatology used by Nolasco *et al*. (in review), which proved to be a fairly good forcing for SD when compared to observations. A preliminary comparison between that climatology and the present

Table 1. List and characteristics of the CGCM used.

Model	Institution/ Country	Land Resolution	Ocean Resolution
CGCM v3 (t47)	CCCMA, Canada	3.75º x 3.71º	1.88º x 1.86º
CNRM-CM v3	CNRM, France	2.81º x 2.79º	2º x 1º
MIROC (medres)	CCSR, NIES and FRCGC, Japan	2.81º x 2.79º	1.41º x 1º
CSIRO Mk3.5	CSIRO, Australia	1.88º x 1.87º	1.88º x 0.93º
GFDL CM2.0	NOAA, USA	2.5º x 2º	1º x 1º
GISS E-R	NASA, USA	5º x 4º	5º x 4º
UKMO HadCM3	Hadley Center, Met Office, UK	3.75º x 2.5º	1.25º x 1.25º
MPI ECHAM5	Max Planck Institute, Germany	1.88º x 1.87º	1º x 1º
CGCM v2.3.2	MRI, Japan	2.81º x 2.79º	2.5º x 2º
Ensemble Mean	---	2.5º x 2.5º	1.25º x 1.25º

ensemble was also carried out, showing reasonable results for the latter as ROMS surface forcing (not shown).

RESULTS AND DISCUSSION

Results will be presented for the monthly means of the last five years of the SD runs, present and future. A seasonal analysis of the sea surface temperature and salinity is carried out, followed by cross-shore sections in depth to 200 m of meridional velocity.

Seasonal Analysis

Figure 2 presents the seasonal evolution of sea surface temperature (SST – left column) and salinity (SSS – right column) for present and future at the five points marked on Figure 1, located at the 100-m isobath. The strongest differences are observed in winter and autumn, and the lowest during spring and summer. SST does not present a sinusoidal-like evolution as expected at more offshore locations. On the contrary, at these points, minimum temperatures are registered between February and April, and a second minimum is reached between June and August. The highest temperatures are observed in autumn, when the northerly winds begin to relax after the upwelling season. These peaks also occur in the future, although enhanced. The SST difference for months May to August is of +1ºC, while for the remaining months the difference is about +2ºC. In October at 40ºN, differences reach +2.5ºC, whereas at 41ºN and 42ºN the lowest differences are found in August and September (0-0.5ºC). Concerning SSS, the general difference between present and future is of -0.2. Moreover, while at present the SSS minimum is reached in July (with the exception of the 42ºN section, where this minimum is observed in September), in the future the lowest SSS is found in May for the southern sections and also in September for the northern sections. May is the month where the future-present difference is the highest, reaching -0.3. The May and September double low peak results in a summer increase of salinity, which, being absent in the present series, means a lower difference (about -0.1) between present and future for these months.

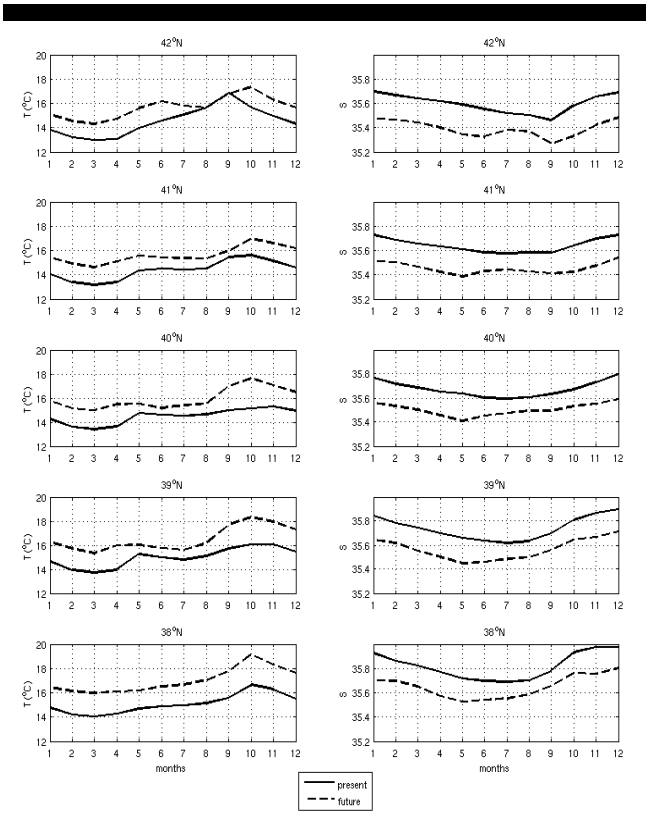

Figure 2. Monthly means of SST (left column) and SSS (right column) at the 5 points depicted on Figure 1, present and future.

From Figure 2 it is evident that the temperature and salinity seasonal evolution depend on latitude, but these variables may also depend on longitude. Monthly mean plots of SST and SSS future minus present differences along longitude are shown on Figure 3, for three latitudinal bands: 41-43ºN, 39-41ºN and 37-39ºN. In what concerns temperature, from a first observation, there is not a striking difference between offshore/near shore locations. At the northern band (Figure 3a), the general difference is of +1 to +1.5ºC. The exception is between July and September, where a difference as low as zero can be found centered at 9.3ºW, the average location of the 100-m isobath at that latitudinal band (see Figure 1), where the upwelling jet is the strongest (as discussed further on). Onshore, differences reach the highest (+2ºC) difference in winter and the lowest (+0.5º) in summer. At the central band (Figure 3c), differences are of mostly +1.5ºC except for the upwelling season (May to September), where they are in general lower, being the lowest (< 0.5ºC) close to the coast. Concerning the southernmost band (Figure 3e), the strongest differences are again around 9.2-9.3ºW, with differences reaching +2-3ºC between August and October. The early summer interval (May-July) is once more the one that presents the lowest SST differences (+1-1.5ºC).

In what concerns salinity (Figure 3b,d,f), the northern band shows strong negative differences offshore between May and November (from -0.25 to -0.35), while near shore during summer differences are again the lowest. At the central band, SSS differences vary in general between -0.15 and -0.2, with differences of less than -0.1 near the coast between June and September. Finally, at the southern band, the coastal summer low differences of about -0.1 are displaced toward offshore longitudes.

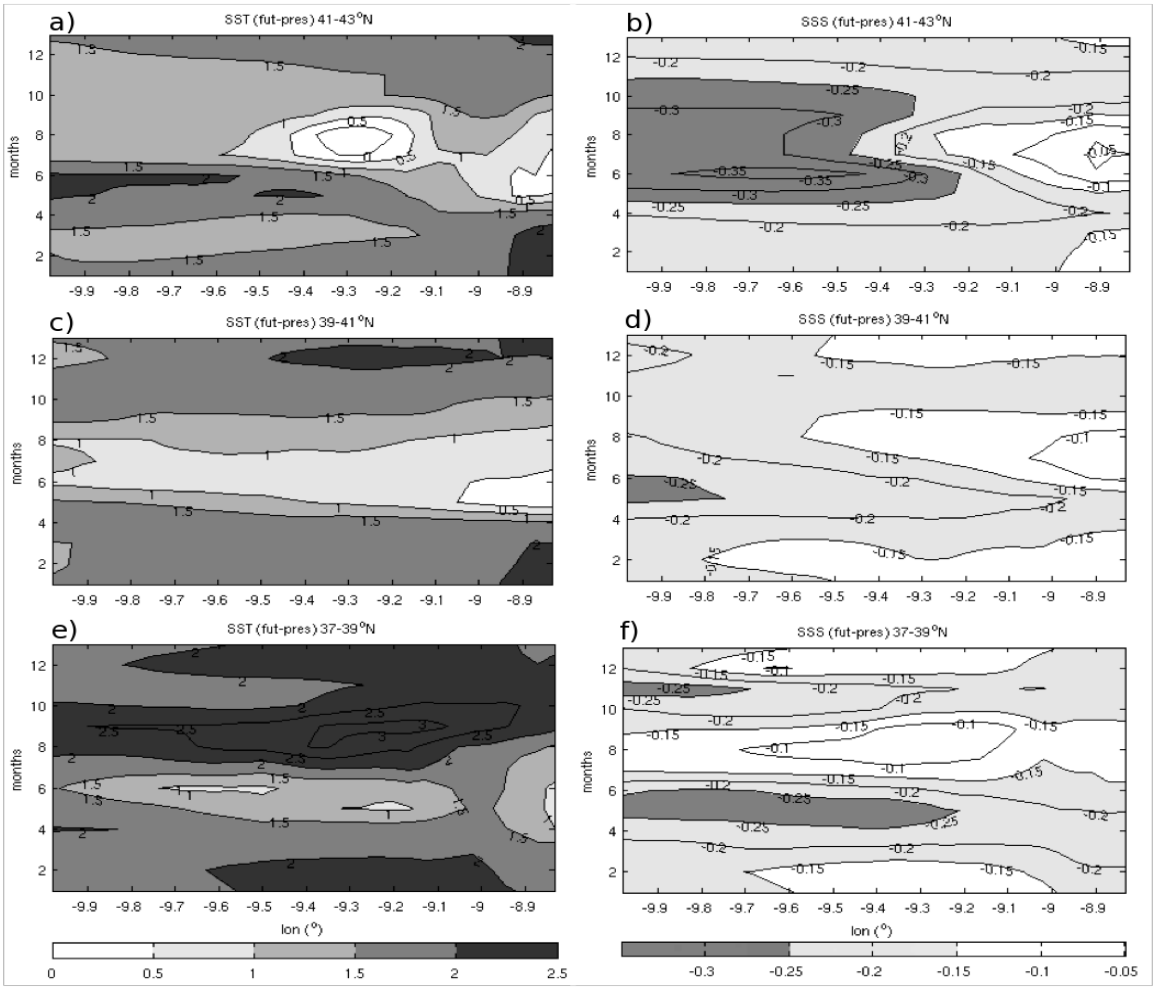

Figure 3. Hovmöller diagrams of future minus present differences of SST (left column) and SSS (right column) for three latitude bands.

From these observations we can draw that, despite the warmer temperatures in about 2ºC and fresher waters in about 0.2 in the future, these differences are smaller near the coast and during the upwelling season. This can mean that upwelling events weaken. It is interesting to note that SST and SSS strong/weak differences do not exactly correspond in time. For instance, the coastal SST minimum differences occur in May-June, while coastal SSS minimum differences occur in July-August.

Cross-shore Sections

Looking further into the upwelling dynamics, Figures 4 and 5 show zonal sections (down to 200 m) of the meridional component of the velocity, superimposed with temperature, for January (Figure 4) and July (Figure 5), at latitudes 42ºN (a,b) and 38ºN (c,d). Left column corresponds to the present run and right column to the future run. Regarding January (Figure 4), the signature of the Iberian Poleward Current (IPC) is evident at 42ºN, reaching 10 cm/s at the shelf/upper slope, delimited by the 13.5ºC isotherm. In the future, this flow seems to be weaker and shallower. The upper 100 m are warmer by about 1.5ºC. This warmer tendency decreases in depth, with a warming of 0.5ºC at 200 m. Farther south, at 38ºN, an equatorward flow appears, down to more than 200 m although not surpassing 5 cm/s. In the future, this equatorward tendency is more restricted to the coast, slightly stronger in velocity and 2ºC warmer. These results are not surprising, since the IPC is more marked in the northern WIM (Peliz *et al*., 2003). The future differences are not significant as far as the meridional velocity is concerned. As for July (Figure 5), we observe the typical strong upwelling-associated equatorward flow. In the future, at the upper slope and down to 60 m as the distance from the coast increases, the temperature rise is of 1ºC, as seen from the upwelled isotherms. The upwelling jet is slightly stronger in the future at the surface – it increases from 25 (30) cm/s to 30 (35) cm/s at 38ºN (42ºN) – but on the other hand it is more trapped to the coast both in width and depth, clearly evident on the southernmost section. This narrowing of the upwelling signature may be associated with the different warming rates between onshore and offshore locations and to an increase in stratification, especially on the upper 50 m. The slightly higher southward velocities may arise from a slight intensification of alongshore winds (not shown).

CONCLUSIONS

Future climate scenarios are in agreement in what concerns a generalized warming throughout the globe, and that will obviously reflect on the oceans.

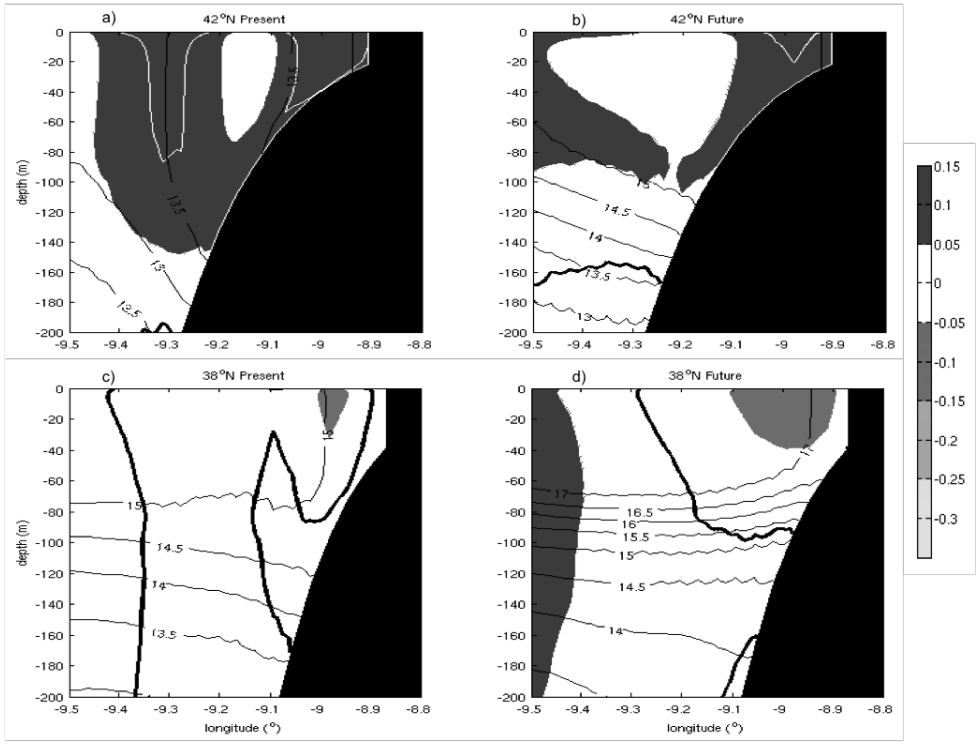

Figure 4. Cross-shore sections at (a,b) 42ºN and (c,d) 38ºN of temperature (black lines) (ºC) and meridional velocity (shading, null velocities marked in thick black lines) (m/s) for January.

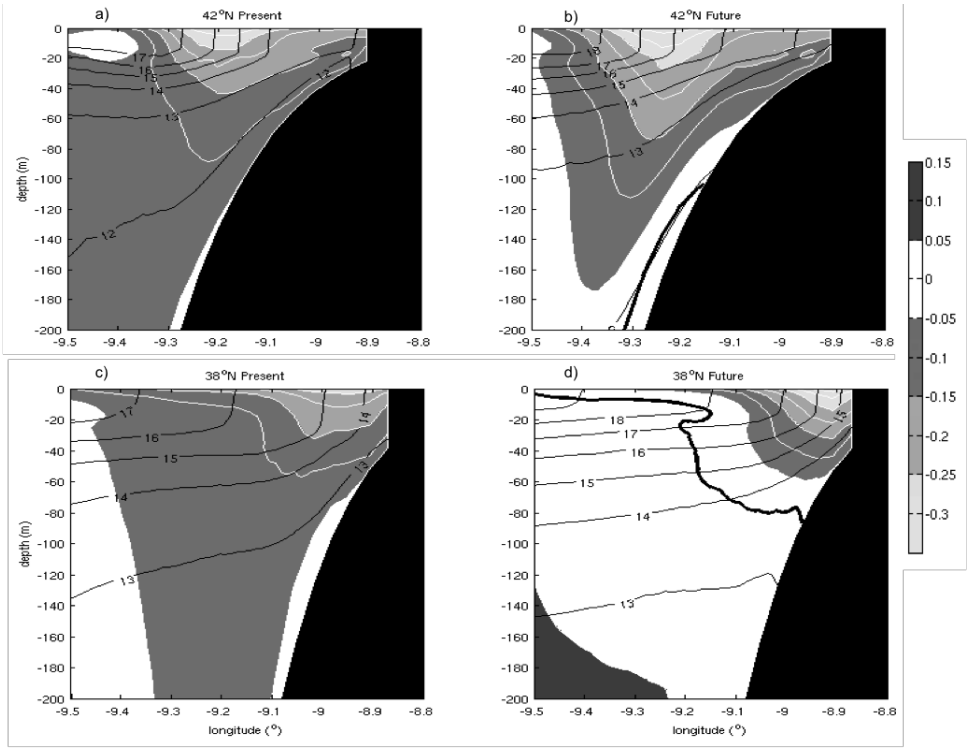

Figure 5. Cross-shore sections at (a,b) 42ºN and (c,d) 38ºN of temperature (black lines) (ºC) and meridional velocity (shading, null velocities marked in thick black lines) (m/s) for July.

On the other hand, global climate models are not too accurate in terms of changes on the marine ecosystems brought about by the increase of greenhouse gas concentration and rising of temperatures. This work aimed at taking advantage of state-of-the-art climate projections and applied it to regional ocean modeling in as optimized a fashion as possible. The ensemble mean is also an effort toward that optimization.

Not surprisingly, the tendency found for the sea surface and subsurface is also a rise in temperatures, accompanied by a decrease in salinity, which is a consequence of the predicted fresh water input in the North Atlantic through melting of the polar regions ice, a characteristic of the IPCC A2 scenario. Nevertheless, since it is an upwelling system, the warming and the freshening of upper layer waters depends on season, latitude and distance to the coast. Our results suggest, first of all, that future-present differences in general are higher in winter than in summer. Close to the coast, SST and SSS differences are lower during the upwelling season than in the remaining months. On the other hand, SST differences tend to be accentuated to the south and SSS differences to the north. Finally, regarding the intensity of the equatorward upwelling-associated jet, according to these simulations, it will be more restricted to the coast in the future, both in width and in depth, which may be explained by the increase of stratification. There is also a slight strengthening of the jet, which may be a consequence of its narrowing.

ACKNOWLEDGEMENTS

A. Cordeiro Pires was supported by Fundação para a Ciência e Tecnologia (FCT) through PhD grant SFRH/BD/47500/2008. R. Nolasco was supported by FCT through programme Ciência 2007.

LITERATURE CITED

Annan, J.D. and Hargreaves, J.C., 2010. Reliability of the CMIP3 ensemble, *Geophysical Research Letters*, 37, L02703.

Antonov, J.I., Seidov, D., Boyer, T.P., Locarnini, R.A., Mishonov, A.V., Garcia, H.E., Baranova, O.K., Zweng, M.M. and Johnson, D.R., 2010. World Ocean Atlas 2009, Volume 2: Salinity. S. Levitus, Ed. *NOAA Atlas NESDIS 69*, U.S. Government Printing Office, Washington, D.C., 184 pp.

Bakun, A., 1990. Global Climate Change and Intensification of Coastal Ocean Upwelling, *Science*.

Barton, E.D., Aristeguí, J., Tett, P., Canton, M., Garcia-Braun, J., Hernandez-Leon, S., Nykjaer, L., Almeida, C., Almunia, J., Ballesteros, S., Basterretxea, G., Escanez, J., Garcia-Weill, L., Hernandez-Guerra, A., Lopez-Laatzen, F., Molina, R., Montero, M.F., Navarro-Perez, E., Rodriguez, J.M., van Lenning, K., Vélez, H. and Wild, K., 1998. The transition zone of the Canary Current upwelling region, *Progress in Oceanography*, 41, 455–504.

Cordeiro Pires, A., Nolasco, R., Dubert, J. and Rocha, A., in prep. Global Climate Models as forcing for regional ocean modeling: A sensitivity study.

Fiúza, A.F.G., 1983. Upwelling patterns off Portugal, *Coastal Upwelling Plenum*, New York.

Holt, J., Wakelin, S., Lowe, J. and Tinker, J., 2010. The potential impacts of climate change on the hydrography of the northwest European continental shelf, *Progress in Oceanography*, 86, 3-4, 361-379.

Lemos, R.T. and Pires, H.O., 2004. The Upwelling Regime off the west Portuguese coast, 1941-2000, *International Journal of Climatology* 24, 511-524.

Locarnini, R.A., Mishonov, A.V., Antonov, J.I., Boyer, T.P., Garcia, H.E., Baranova, O.K., Zweng, M.M. and Johnson, D.R., 2010. World Ocean Atlas 2009, Volume 1: Temperature. S. Levitus, Ed. *NOAA Atlas NESDIS 68*, U.S. Government Printing Office, Washington, D.C., 184 pp.

Miranda, P.M.A., Alves, J.M.R. and Serra, N., 2012. Climate change and upwelling: response of Iberian upwelling to atmospheric forcing in a regional climate scenario, *Climate Dynamics*, doi: 10.1007/s00382-012-1442-9.

Mote, P.W. and Mantua, N.J., 2002. Coastal upwelling in a warmer future, *Geophysical Research Letters*, 29, 23, 2138.

Nakicenovic, N., Alcamo, J., Davis, G., de Vries, B., Fenhann, J., Gaffin, S., Gregory, K., Grubler, A., Jung, T.Y., Kram, T., La Rovere, E.L., Michaelis, L., Mori, S., Morita, T., Pepper, W., Pitcher, H.M., Price, L., Riahi, K., Roehrl, A., Rogner, H.-H., Sankovski, A., Schlesinger, M., Shukla, P., Smith, S.J., Swart, R., van Rooijen, S., Victor, N. and Dadi, Z., 2000. Special Report on Emissions Scenarios: A Special Report of Working Group III of the Intergovernmental Panel on Climate Change, *Cambridge University Press*, Cambridge, U.K., 599 pp.

Nolasco, R., Cordeiro Pires, A., Cordeiro, N., Le Cann, B. and Dubert, J., in review. A high-resolution modeling study of the Western Iberian Margin mean and seasonal upper ocean circulation, *Ocean Dynamics*.

Oliveira, P.B., Nolasco, R., Dubert, J., Moita, T. and Peliz, A., 2009. Surface temperature, chlorophyll and advection patterns during a summer upwelling event off central Portugal, *Continental Shelf Research*, 29, 759–774.

Pauly, D. and Christensen, V., 1995. Primary production required to sustain global fisheries, *Nature*, 374, 255-257.

Peliz, A., Dubert, J., Haidvogel, D.B. and Le Cann, B., 2003. Generation and unstable evolution of a density-driven Eastern Poleward Current: The Iberian Poleward Current, *Journal of Geophysical Research*, 108, C8, 3268.

Peliz, A., Dubert, J., Marchesiello, P. and Teles-Machado, A., 2007. Surface circulation in the Gulf of Cadiz: Model and mean flow structure, *Journal of Geophysical Research*, 112, C11015.

Peliz, A., Rosa, T.L., Santos, A.M.P. and Pissarra, J.L., 2002. Fronts, jets, and counter-flows in the Western Iberian upwelling system, *Journal of Marine Systems*, 35, 61-77.

Perez, F.F., Padin, X.A., Pazos, Y., Gilcoto, M., Cabanas, M., Pardo, P.C., Doval, M.D. and Farina-Bustos, L., 2010. Plankton response to weakening of the Iberian coastal upwelling, *Global Change Biology*, 16, 1258–1267.

Relvas, P., Luis, J. and Santos, A.M.P., 2009. Importance of the mesoscale in the decadal changes observed in the northern Canary upwelling system, *Geophysical Research Letters*, 36, L22601.

Santos, A.M.P., Kasmin, A.S. and Peliz, A., 2005. Decadal changes in the Canary upwelling system as revealed by satellite observations: Their impact on productivity, *Journal of Marine Research*, 63, 359–379.

Shchepetkin, A.F. and McWilliams, J.C., 2005. The regional oceanic modeling system (ROMS): a split-explicit, free-surface, topography-following-coordinate oceanic model, *Ocean Modelling*, 9, 4, 347-404.

Snyder, M.A., Sloan, L.C., Diffenbaugh, N.S. and Bell, J.L., 2003. Future climate change and upwelling in the California Current, *Geophysical Research Letters*, 30, 15, 1823.

Torres, R. and Barton, E.D., 2007. Onset of the Iberian upwelling along the Galician coast, *Continental Shelf Research,* 27, 1759–1778.

Wooster, W.S., Bakun, A. and McLain, D.R., 1976. The seasonal upwelling cycle along the eastern boundary of the North Atlantic, *Journal of Marine Research*, 34, 131−141.